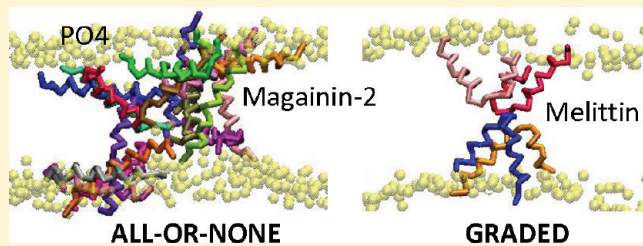


# Difference between Magainin-2 and Melittin Assemblies in Phosphatidylcholine Bilayers: Results from Coarse-Grained Simulations

Kolattukudy P. Santo and Max L. Berkowitz\*

Department of Chemistry, University of North Carolina at Chapel Hill, Chapel Hill, North Carolina 27599, United States

**ABSTRACT:** We performed coarse-grained computer simulations using MARTINI force field to study the difference in the self-assembly and possible pore creation in DPPC phospholipid membranes by two different antimicrobial peptides: magainin-2 and melittin. Simulations showed that magainin-2 peptides create large sized disordered toroidal pores that allow easy water permeation across them. Melittin assemblies contain peptides in U-shaped conformations that, although creating holes in membranes, block effectively the passage of water. These observed structures are consistent with the dye efflux experiments performed on vesicles exposed to solutions containing antimicrobial peptides.



## INTRODUCTION

Although we are aware of the existence of the antimicrobial peptides (AMP) for quite some time, their mechanism of action is still not understood.<sup>1</sup> Many of AMPs have a common feature of being amphipathic and adopting an  $\alpha$ -helical configuration while adsorbed on the lipid membrane surface; they accomplish their mission by disrupting the membrane of the bacteria. Nevertheless, the way different antimicrobial peptides achieve their goal appears to be different. Various models were proposed to explain the function of the peptides, including barrel-stave,<sup>2</sup> toroidal pore,<sup>3</sup> sinking raft,<sup>4</sup> and carpet models.<sup>5</sup> In both barrel-stave and toroidal pore models the peptides create pores in membranes through which the content of the cell can leak. While in barrel-stave pores the walls of the pores contain only peptides, in toroidal pores the lipids of the membranes bend and are parts of the pore walls. It is very hard to gain structural information on the architecture of the pores by using well-established experimental techniques, such as X-ray scattering,<sup>6</sup> and therefore the information needs to be inferred from other experiments, like release of the dye from the lipid vesicle after expose of the vesicle to the presence of AMP.<sup>7</sup> Particularly useful information is gained from the experiments performed on the giant unilamellar vesicles (GUVs). Thus, while it was presumed for some time that melittin and magainin-2, the two well-studied AMPs, create toroidal pores in the membranes,<sup>8</sup> and therefore their action is quite similar, the experiments with GUV indicated that this may not be the case.<sup>7</sup> From these experiments it was observed that, while melittin induces graded dye release, magainin-2 induces all-or-none release. Almeida and Pokorny proposed a detailed description of the two mechanisms of the dye release.<sup>7</sup> According to their description, the initial step for both mechanisms represents adsorption of the peptide from the aqueous solution to the surface of the vesicle and a structural transition from the coil to an  $\alpha$ -helical

configuration. After this initial common step, the two mechanisms resulting in the dye release differ. In the all-or-none mechanism pores are formed in the membranes, initiated by tension due to the presence of peptides. These pores may be stabilized by the presence of peptides, although it is not required that the pores have an organized character, like the one depicted in an idealized toroidal pore representation. As a matter of fact, molecular dynamics (MD) simulations showed that pores have a "chaotic" disorganized shape.<sup>9</sup> It is possible that some peptides translocate across the pore, but this kind of action is not needed to explain the all-or-none mechanism. Nevertheless, such translocation can occur, as it was proposed to happen in the case of magainin-2. When the graded mechanism is operational, AMPs insert into membrane with higher probability and create a transient pore, causing an efflux of the dye. Eventually, peptides translocate across the membrane, create an equilibrium population of the peptides, mass balance is restored, and the dye efflux diminishes or even stops. Almeida and Pokorny postulated that the mechanism of dye release, or AMP action, all-or-none or graded, will depend on the ease of AMP insertion and therefore on the thermodynamics of this process. Further tests of this hypothesis performed by the same group showed that this is not the case.<sup>10</sup>

Molecular dynamics computer simulations usually play a very important role when structural information about biomolecular systems needs to be refined or when dynamical information needs to be obtained. Simulations that used molecular detailed description of AMP and lipid bilayers were also performed, including AMPs such as magainin-2 (or close relative of this peptide) and melittin. Detailed MD simulations on the

Received: December 13, 2011

Revised: January 30, 2012

Published: February 3, 2012



analogue of magainin-2 peptide, magainin-H2, interacting with the DPPC bilayers showed that these peptides form disordered toroidal pores at a sufficient peptide/lipid concentration.<sup>11</sup> (Magainin-H2 was chosen due to its ability to form pores in DPPC more easily because it has a higher hydrophobic moment compared to magainin-2.) The simulations were done on systems containing up to 4 peptides and a bilayer consisting of 128 DPPC molecules. In these simulations a 2 nm wide pore was obtained when the peptide/lipid ratio was 4/128. The same group also studied melittin action on bilayers consisting of 128 and 512 DPPC molecules and again observed a spontaneous formation of pores consistent with the disordered pore model.<sup>9</sup> Although disordered toroidal pores were observed in both cases, it must be noted that the time scales of these detailed simulations (up to 250 ns) were not long enough to distinguish between the structural differences in pores formed by these peptides. Moreover, because of the time scale limitation, it is not known if the observed disordered pores represent a transient phenomenon during which peptides translocate across the membrane. Therefore, in some other simulations it was presumed that after a transient period pores in membranes may assume regular shapes, and therefore structures of pores that have walls lined up with AMPs were investigated by inserting peptides, such as melittin, into initially prepared cylindrical pores in the membranes.<sup>12–14</sup> It was observed that a regular toroidal pore can be created by four melittins, if the arrangement of these four melittins that are parts of the initially prepared cylindrical pore is symmetrical: that is two of the peptides have their C-termini anchored to one side of the bilayer, while the other two peptides have their C-termini anchored to the other side of the bilayer.<sup>14</sup>

Unfortunately, because of a very short time step employed in detailed MD simulations (1–2 fs) and a large number of atoms needed to depict the biological system, MD simulations that use atomic detailed description of the force field, in most cases, cannot be used to study systems larger in size than few tens of nanometers over periods of time longer than few hundred nanoseconds (recent advances in hardware promise to overcome some of these restrictions<sup>15</sup>). Today, to avoid the restrictions on both time and spatial scales imposed by the use of the detailed force fields in molecular dynamics simulations, coarse-grained (CG) models are used. By coarse-graining the system, one can speed up the time step of the simulation, so the simulations can be performed over time periods of microseconds. CG also reduces the number of particles, thus increasing the spatial domain of the system under the simulation.

Naturally, CG methodology is intensely used in the studies of membranes and also in the study of AMPs interacting with membranes, since one needs to observe these systems over longer time and larger space domains. Thus, simulations performed with a CG force field MARTINI<sup>16</sup> confirmed the existence of the disordered toroidal pores formed by magainin-H2<sup>17</sup> and showed that the pores were stable for longer times<sup>18</sup> (compared to typical time periods that pores were investigated in molecular detailed simulations). Gkaka and Sarkisov<sup>19</sup> also used coarse-grained MARTINI force field to perform simulations on different peptides interacting with the DPPC membrane, and they also observed pore formation by magainin-H2 peptide. More recently, Woo and Wallqvist<sup>20</sup> used MARTINI to perform coarse-grained simulations on magainin-2 peptides interacting with a mesoscale patch of a membrane containing a mixture of zwitterionic and anionic lipids, and again they observed creation of disordered pores in case when some of the

peptides were partitioned into the bilayer interior in a transmembrane orientation. Notice that in all the above-mentioned coarse-grained simulations, some of the peptides were initially placed into the membrane interior in the transmembrane orientation. Interestingly, no results seem to exist in the literature regarding CG simulations of bilayers with melittin.

As we can see, previous detailed or CG simulations do not provide us with an explanation why there is a difference between magainin and melittin: why one is promoting all-or-none efflux of the dye from a vesicle, while the other is promoting a graded efflux. The goal of the present work is to use the CG simulations and extract some structural information about the difference in action between melittin and magainin, specifically magainin-2.

## METHODS

The two types of peptides used in this study are 26-residue melittin (GIGAVLKVLTTGLPALISWIKRKRQQ) and a 23-residue magainin-2 (GIGKFLHSACKFGKAFVGEIMNS). The net charge of melittin depending on whether the N-terminus is protonated or not is +6 or +5, although at physiological conditions the N-terminus residue GLY is reported to be protonated.<sup>21</sup> In our simulations we consider melittin to have charge +6 with four charges residing on the sequence of four residues -LYS-ARG-LYS-ARG- that are close to the C-terminus, one charge residing on the protonated N-terminus GLY, and the remaining charge is on the LYS at residue 7. The charge of magainin-2 peptide is +3, and this charge is not concentrated closely to termini. The lipid membrane consisted of 512 dipalmitoylphosphatidylcholine (DPPC) molecules. Na<sup>+</sup> and Cl<sup>-</sup> ions were added to the system in order to make the solvent a 0.1 M NaCl solution and also to neutralize the charge on the peptides. The simulations were performed using GROMACS<sup>22</sup> software package with the MARTINI force field where molecules are represented as CG groups.

The lipid membrane was constructed in the following way: an equilibrated bilayer consisting of 128 DPPC molecules was downloaded from the MARTINI Web site ([www.mdt.chem.rug.nl/cgmartini/](http://www.mdt.chem.rug.nl/cgmartini/)), and it was replicated twice in X and Y directions in the plane of the membrane to get a bilayer consisting of 512 DPPC molecules. This system was energy-minimized and solvated with water, followed by energy minimization and NPT simulation for 60 ns, to obtain a well-equilibrated bilayer.

The equilibrated bilayer was placed at the center of the simulation box, and peptides, initially oriented parallel to the membrane plane, were distributed in the bilayer interfacial region, so that their centers of mass were at distance ~1.4 nm from the bilayer center. The proteins were placed uniformly, parallel to each other, 1.5 nm apart in the X direction, so that their hydrophobic sides were facing the bilayer interior. (However, additional simulations demonstrated that final results were qualitatively unaffected by placing proteins further apart, or closer to each other, or even by placing them with their hydrophobic sides not facing the bilayer interior.)

This protein/bilayer system was energy minimized and then solvated with water and ions. After performing these steps, we obtained our initial systems containing lipids, water, proteins, and ions. The densities of the system components displayed a broad distribution for the particles of the coarse-grained peptides with the center of the distribution located between the distributions for the phosphate and glycerol groups of the coarse-grained bilayer. Experimental studies showed that

melittin density distribution is also represented by a broad peak situated between the peaks of phosphate and carbonyl regions with melittin helix axis located at a distance 1.75 nm from the bilayer center.<sup>23</sup> In case of magainin-2 experiments showed that it also permeated into the bilayer interface region. Thus, it was reported that Trp residue of the FSW-magainin-2 was located

at distance 1 nm from the bilayer center.<sup>24</sup> Such observed penetration of peptides into the inner part of the bilayer interface face is also consistent with the sinking raft hypothesis.

We also ran simulations with the initial placement of our peptides at the outer surface of the lipid bilayer but did not observe any permeation of the peptides into the depth of the bilayer interfacial region. This may be due to some problems with the MARTINI force field that imposes large penalties on the desolvation of the peptide. To understand better the location of peptides in the bilayer interface and their structure, detailed calculations on free energies using atomistic force fields have to be performed, and we are in a process of performing them.

Since our peptides were initially placed at the interface region, we chose their structure to be helical, as indicated by the experiments. Therefore, the initial structure of melittin corresponds to the crystal structure<sup>25,26</sup> (PDB ID: 2MLT) that can be considered to contain two helices consisting of 9 and 14 residues separated by a kink at the position of the Pro residue, whereas the initial magainin-2 structure corresponds to its NMR structure in micelles<sup>27</sup> (PDB ID: 2MAG) that displays a single helix consisting of 18 residues. Because of the specifics of the MARTINI force field, this secondary structure remained unchanged during the simulations.

In our simulations we considered systems with different numbers of peptides. The content of these systems including the number of molecules in each system is given in Table 1. As the table shows, we considered three different P/L ratios: 6/512, 12/512, and 24/512. In ten simulations peptides were

**Table 1. Compositions and Simulation Lengths of the Systems<sup>a</sup>**

system	protein	no. of proteins side 1/side 2	no. of Na <sup>+</sup> /Cl <sup>-</sup>	no. of CG waters	simulation length (μs)
I-A	magainin-2	6/0	91/109	12 284	2.1
II-A	magainin-2	12/0	90/126	12 122	2.1
III-A	magainin-2	24/0	89/161	11 874	8.2
IV-A	magainin-2	6/6	89/125	12 092	2.1
V-A	magainin-2	12/12	88/160	11 844	9.9
I-B	melittin	6/0	91/127	12 258	2.1
II-B	melittin	12/0	90/162	12 077	2.1
III-B	melittin	24/0	88/232	11 710	6.3
IV-B	melittin	6/6	90/162	12 120	2.1
V-B	melittin	12/12	88/232	11 748	4.2
VI-Ba	melittin	9/9 (6) <sup>b</sup>	86/230	11 508	2.0
VI-Bb	melittin	9/9 (6) <sup>b</sup>	86/230	11 633	2.0

<sup>a</sup>All systems contain phospholipid bilayers with 512 DPPC molecules. Simulation length corresponds to the total simulation time of the system. <sup>b</sup>In simulations VI-Ba and VI-Bb, six peptides were initially placed in a transmembrane configuration.

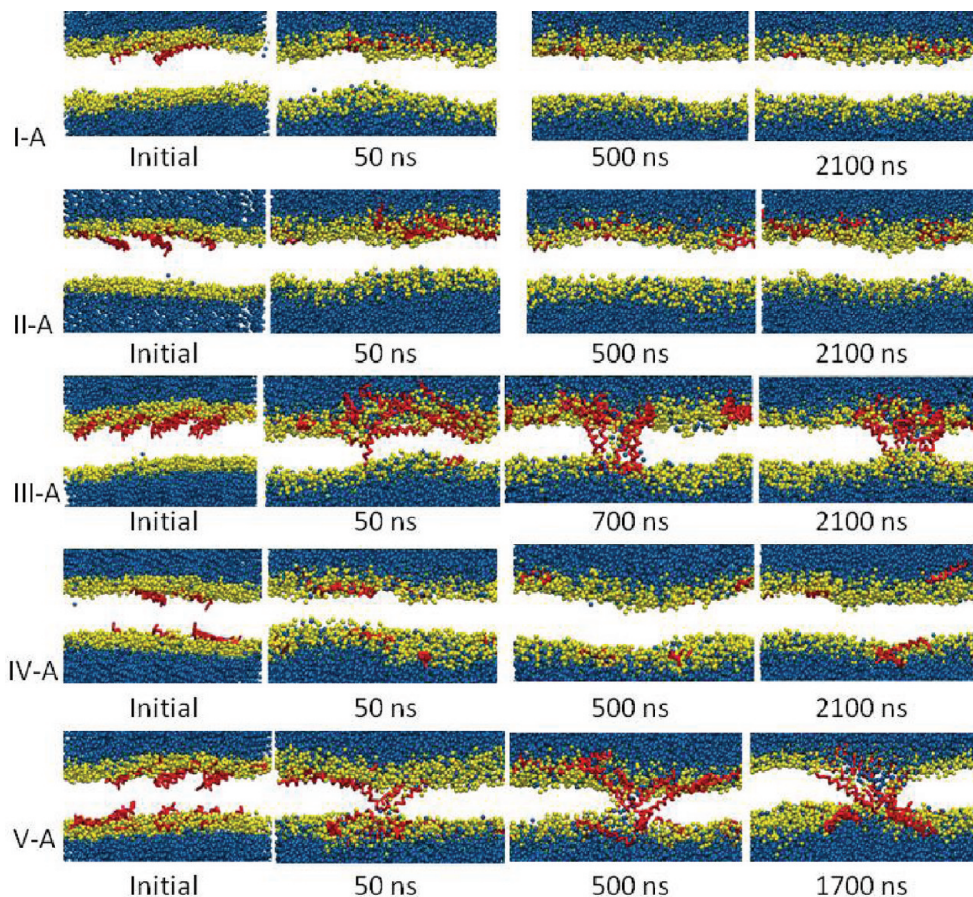


**Figure 1.** Time evolution of systems containing magainin-2 peptides. System specifications are given in Table 1. CG water molecules are shown as blue beads, lipid head groups as yellow beads, and proteins in red. For clarity, only protein backbones are shown and lipid tails are not shown. The time of the snapshots is also shown.

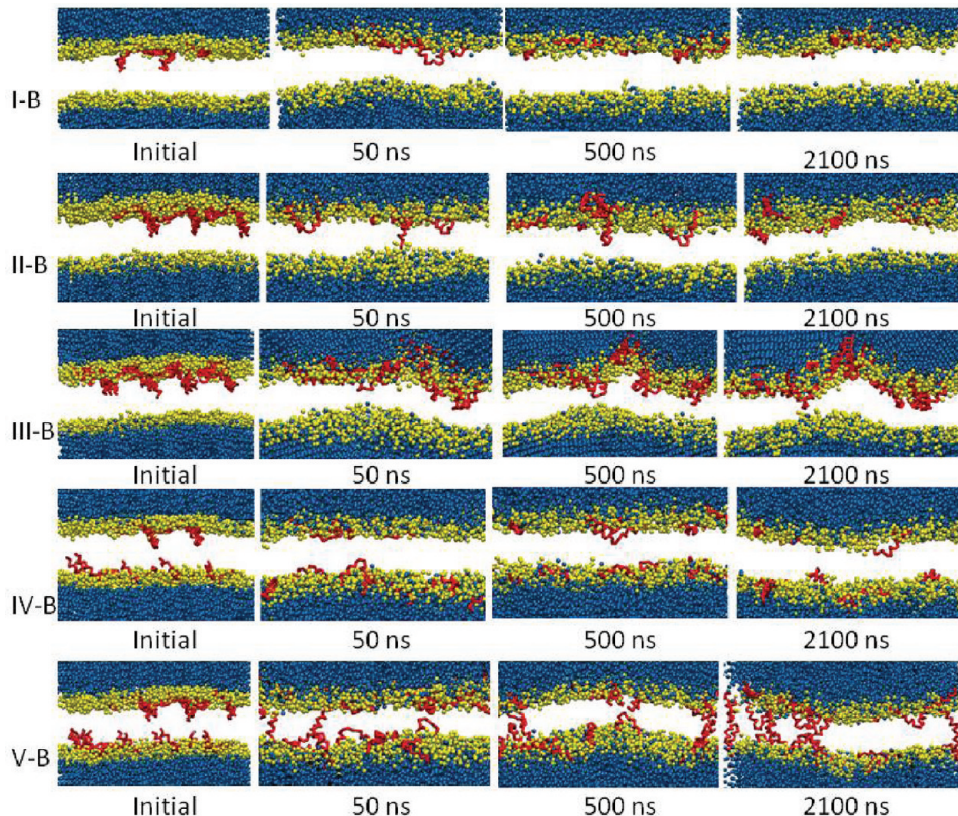


**Figure 2.** Time evolution of melittin systems (I–V) with system specifications given in Table 1. The color code and notations are as in Figure 1.

initially placed parallel to membrane–water interface, either on the same side (leaflet) of the membrane or on both sides. Five systems were initially studied for each peptide, with magainin-2 systems denoted as A and melittin systems denoted as B. Thus, systems I, II, and III correspond to asymmetric arrangement in which proteins were placed only on one side of the membrane, side1. Systems IV and V correspond to the symmetric arrangement when proteins were placed on both sides in equal numbers. In the case of melittin two additional systems (VI-Ba, VI-Bb), with the P/L ratio 24/512, were also studied. In these systems 6 of the 24 melittins were initially placed in the transmembrane (TM) orientation perpendicular to the membrane plane. The rest of 18 peptides were placed on the two sides of the membrane, so each side contained 9 peptides placed near the membrane–water interface in an orientation parallel to the membrane. In system VI-Ba, the TM peptides were placed 4 and 3 nm apart in X and Y directions, respectively, while in the case of VI-Bb the peptides were placed closer, with the separation between them being 2 and 1.5 nm respectively in the X and Y directions. The bilayer–peptide systems were energy-minimized using steepest descent method to remove the unphysical contacts.

Most of our initial systems, shown in Figures 1 and 2 (see columns designated initial), were further energy-minimized and equilibrated using position restraints on peptides for 6 ns. No position-restrained simulations were done for systems VI-Ba and VI-Bb. Finally every system was simulated using the constant number of particles, pressure, and temperature (*NPT*) ensemble. The *NPT* simulations were performed using Berendsen<sup>28</sup> temperature coupling scheme with temperature at 323 K and semi-isotropic pressure coupling scheme at 1 bar using the Parrinello–Rahman scheme.<sup>29</sup> The pressure coupling

relaxation time was taken to be 3.0 ps and the compressibility value  $4.5 \times 10^{-5} \text{ bar}^{-1}$ . Periodic boundary conditions were employed. The time steps for the MD simulations were 0.02 ps for the position-restrained simulations and 0.03 ps for the production runs. Nonbonded interactions were cut off at 1.2 nm according to protocols recommended for the use of MARTINI force field. The initial sizes of all systems were 12.4, 12.8, and 15.0 nm in the X, Y, and Z directions, respectively. System configurations were visualized using the VMD software package.<sup>30</sup>

## RESULTS

**Magainin-2 Forms Water-Filled Toroidal Pores.** The simulations with magainin-2 were performed for five different systems (I-A, II-A, III-A, IV-A, and V-A) corresponding to three different P/L ratios: 6/512, 12/512, and 24/512, as described in Table 1. A critical peptide concentration is required for the peptide to disrupt the membrane. For magainin-2 it was proposed that a critical P/L ratio is in the range of 1/100 to 1/30.<sup>31</sup> However, recent experiments<sup>32</sup> indicated that it is the concentration of the peptide in the bilayer rather than in the bulk that determines the rate of pore formation; therefore, it was suggested that the critical peptide concentration is closer to ~1/20. Our simulations are within the range of these P/L ratios. Also, it should be noted that the correct dependence of pore formation on the P/L ratio may not be reproduced accurately by a CG model. In three of our systems (I, II, III), the peptides were placed just on one side of the bilayer near the membrane–water interface, mimicking an asymmetric binding of peptides to the bilayer surface, while in the other two systems peptides were placed in equal numbers on both sides, mimicking a symmetric surface attachment, that can occur after

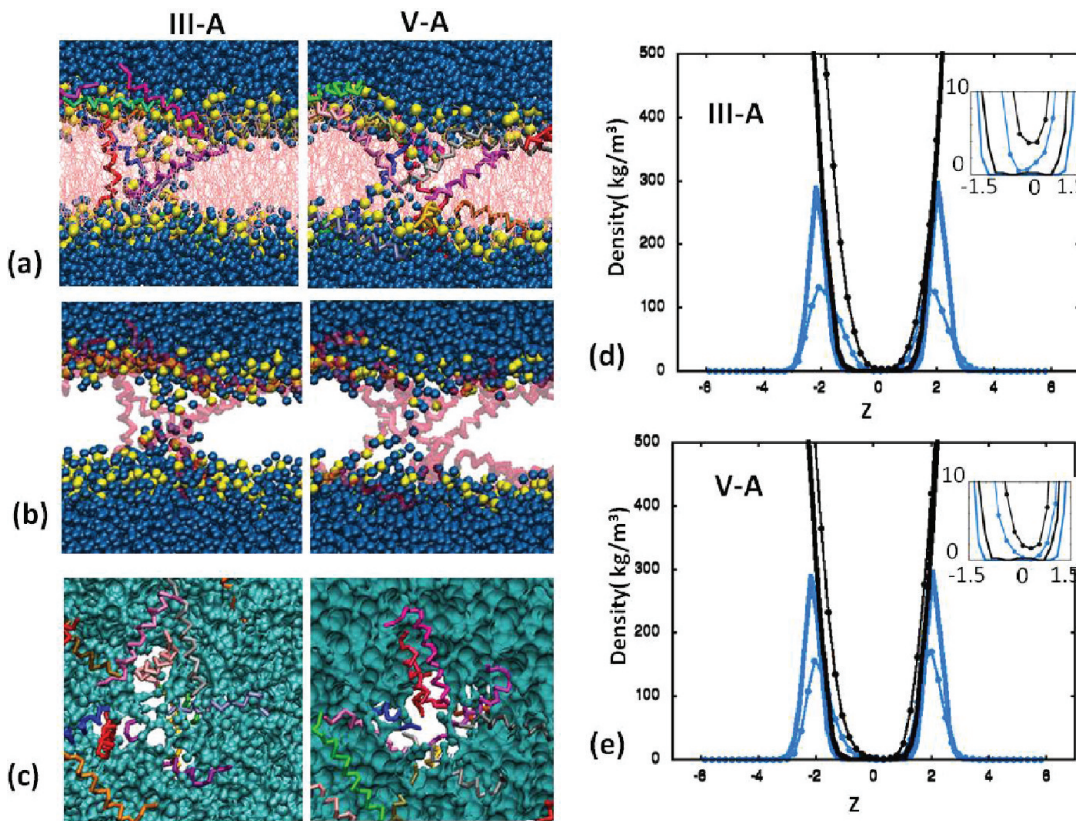


**Figure 3.** Magainin-2 pores formed in systems III-A and V-A. Water-filled, toroidal pores are formed spontaneously in both cases. The snapshots correspond to 600 ns for system III-A and 500 ns for V-A. (a) Side view of the pores. Blue beads are CG waters and yellow beads are the phosphate groups. Backbones in different colors represent individual proteins. DPPC molecules are shown as pink lines. (b) Like in (a), only without DPPC tails to show more clearly the presence of water and phosphate groups inside the pore. (c) Top view of the pores. The DPPC membrane is shown as a solid surface and peptides are in different colors. (d, e) Partial densities of phosphate groups (blue) and water (black). Solid lines represent densities corresponding to pure DPPC bilayer while lines with circles correspond to membranes with pores. Insets clearly show presence of water inside the membrane. More water is present in the membrane in asymmetric case (III-A) than in the symmetric case (V-A).

some of the peptides translocate across membrane. All peptides were initially placed parallel to the bilayer plane and were partially inserted into the hydrophobic interior of the membrane with the hydrophobic side facing the bilayer interior. The time evolutions of these systems are shown in Figure 1. As is shown in this figure, no pores were observed when the P/L ratios were 6/512 or 12/512 in both symmetric and asymmetric cases (systems I-A, II-A, and IV-A) during the 2.1  $\mu$ s of the MD run. However, pores were observed for the runs with the P/L ratio of 24/512 in both symmetric and asymmetric cases. In the asymmetric case III-A 24 peptides were initially placed on side 1 of the bilayer, and after the beginning of the simulation the peptides started crossing the bilayer interior by penetrating the membrane in a transmembrane orientation, perpendicular to the bilayer plane. As shown in Figure 1, in the system III-A already after 50 ns, one peptide got translocated to the side 2, and another peptide reoriented into the transmembrane configuration. As the time progressed, more and more peptides aggregated in the transmembrane orientation, and a toroidal pore containing permeating water was formed at about 600 ns of the run. In the symmetric case, pores were formed in a similar fashion, but faster than in the asymmetric case. The structures of these pores are shown in more detail in Figure 3. Figures 3a and 3b show side views of the pores formed in cases III-A and V-A. For the asymmetric case III-A the snapshot shows the pore at 600 ns with the peptides oriented in a transmembrane fashion, connecting with both

leaflets of the bilayer. As Figures 3a and 3b show, the peptides are arranged in a similar way for the symmetric case V-A; the snapshot depicted is made at 500 ns. Figure 3b shows the presence of water in the pore, bending of the lipids, and presence of the phosphate groups in the pore interior, revealing the toroidal nature of the pore in both asymmetric and symmetric cases. The top view of the pores shown in Figure 3c indicates that peptide distribution around the pore is rather disordered. Overall, the CG results seem to be consistent with the disordered toroidal pore model proposed for magainin-2 on the grounds of atomistic studies.<sup>11</sup> More details about the toroidal character of the pores and presence of water in these pores can be inferred from Figures 3d and 3e where we display the density profiles of the phosphate group and water in systems III-A and V-A. We compare these densities with the corresponding densities obtained from simulations of the pure DPPC bilayer. The insets in each figure provide a closer view of the profiles and clearly show the presence of water and phosphate groups toward the center of the bilayers. Interestingly, more water (almost 2 times more) is present in the asymmetric case than in the symmetric case. We speculate that the membrane in the asymmetric case is more stressed until the pore is formed and peptides translocate to the other side of the bilayer, and therefore, more water can penetrate initially into the pore. Long time behavior of these systems is depicted in Figure 4. Figures 4a and 4c present the side views of the pores at different times. In the case of system III-A the water-filled

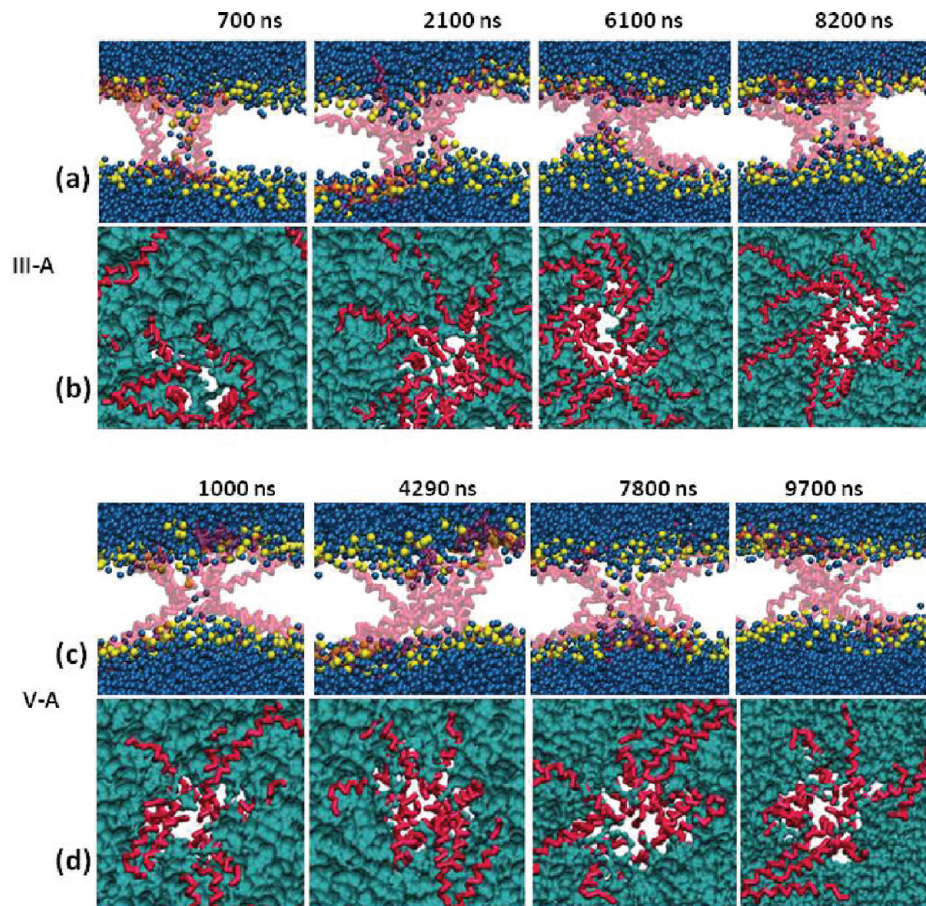


**Figure 4.** Long time behavior of magainin-2 pores. (a) and (c) show side views of the pores at different times for systems III-A and V-A, respectively, while (b) and (d) show top views. Proteins are shown in red, water as blue beads, and  $\text{PO}_4$  groups as yellow beads. The DPPC membrane is shown as cyan solid surface. Notice that more water is present inside the pore in the asymmetric case III-A than in the symmetric case V-A.

nature of the pore is maintained until  $8.2 \mu\text{s}$  of the run. However, in system V-A the pores tend to be less watery or tend to close transiently. The top views of the systems depicted in Figures 4b and 4d show that, once the pore is formed, peptides continue to aggregate in the pore region. The figures indicate that nearly all peptides moved to the pore region by  $2\text{--}4 \mu\text{s}$  of the run. We also estimated the sizes of the pores created by magainin-2 peptides. The pore size was considered to be the diameter of the circle that fits to the glycerol–water interface of the pore.<sup>11</sup> The size of the pore in the asymmetric case III-A is the largest, and it is  $\sim 5 \text{ nm}$ . In the symmetric case V-A the pore size is smaller, and it is  $\sim 3 \text{ nm}$ .

**Melittin Makes Holes That Are Not Well-Defined Channels.** Five systems corresponding to the systems studied for magainin-2, having the same P/L ratios and initial distributions, were also studied for melittin. Therefore, a direct comparison between the actions of the two peptides on the membrane can be made. Additionally, two more systems were also studied for melittin, with the P/L ratio of 24/512 so that 6 out of the 24 peptides were initially placed in the TM orientation. Thus, altogether seven systems containing melittin AMP were studied, as described in Table 1; they were named I-B, II-B, III-B, IV-B, V-B, VI-Ba, and VI-Bb according to the P/L ratio and the initial arrangement of the peptides. The time evolutions of systems I–V are shown in Figure 2. None of these systems showed formation of a well-defined pore. In system III-B, containing 24 peptides initially placed on side 1 of the

bilayer, melittin was found to induce micellization of the bilayer. This micellization is depicted in Figure 5a. The figure shows that during the micellization the tails of the lipid molecules are found to bulge out from the bilayer. We also observed that a more substantial micellization of the bilayer induced by the presence of melittin was obtained in simulations with slightly different initial conditions. In system V-B, which corresponds to the symmetric arrangement of the peptide and the P/L ratio of 24/512 (12 peptides in each leaflet), melittin formed multiple aggregates in the membrane interior and the side view of them can be seen in Figure 5b depicting a snapshot (taken at  $4.2 \mu\text{s}$ ) of the system. These aggregates do not represent well-defined channels; they are just transmembrane aggregates of 4–6 melittin peptides, with each of the peptides adopting an U-shaped conformation. This conformation is due to the melittin bending at large angles about the kink at the proline residue, so that both termini residues of the peptide are attached to the same leaflet of the bilayer. A similar U-shaped conformation adopted by influenza virus M2-TMP peptide in a phospholipid bilayer was observed in simulations of Yeh et al.<sup>33</sup> Interestingly, the assembly of U-shaped melittin peptides occurs on both leaflets of the bilayer in the same location, thus creating a hole in the membrane through which slight permeation of water exists. The size of the holes is  $\sim 2 \text{ nm}$ , smaller than the size of the holes created by magainin-2; it is important to remember that the hole is obstructed by the U-shaped peptides. We also did not observe the

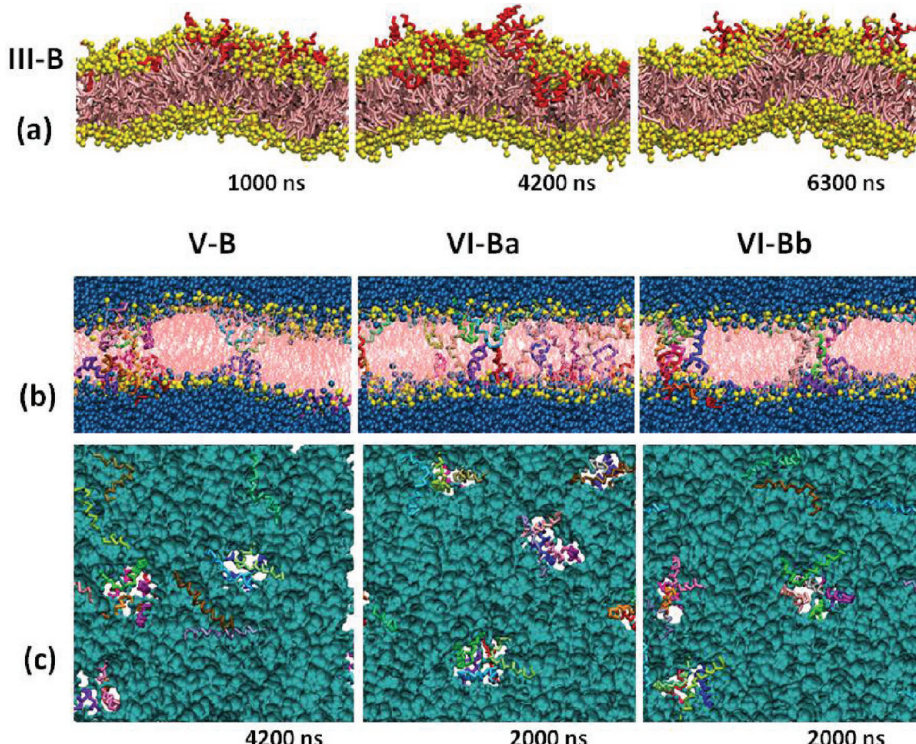


**Figure 5.** Melittin action on the bilayer. (a) Melittin peptides, initially placed on one side of the bilayer tend to micellize the bilayer at high P/L ratios (III-A, P/L ratio = 24/512). The head groups are shown as yellow beads. The lipid tails are shown in pink and the protein backbones are shown in red. (b) Side views of the symmetric melittin systems at high P/L ratio (24/512). Unlike magainin, melittin forms multiple aggregates with 4–6 peptides. (c) Top view of the systems. Melittin aggregation inside the membrane leads to creation of small holes in the bilayer. The color codes are the same as in Figure 3.

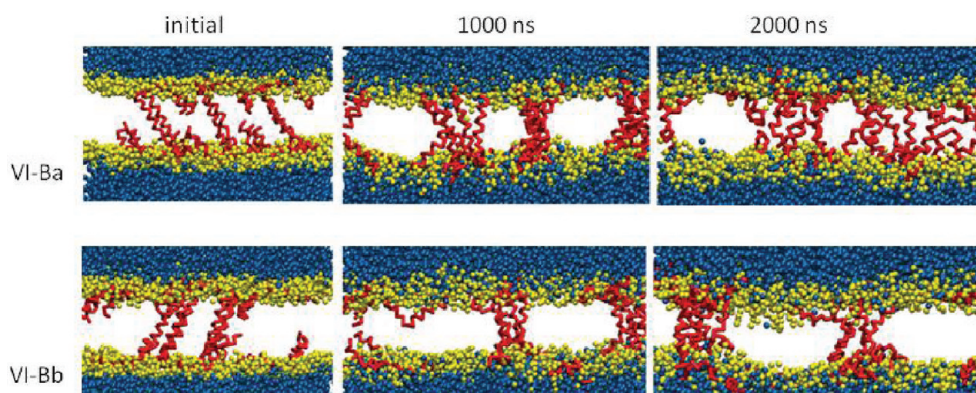


**Figure 6.** Time evolution of melittin systems with initial states containing peptides in the transmembrane (TM) orientation. TM peptides are placed closer to each other in VI-Bb than in VI-Ba to promote aggregation. Blue beads represent CG water, yellow beads represent head groups, and protein backbones are shown in red. Beads are not to scale.

appearance of phosphate groups in the holes created by melittin. We show the top view of the case V-B system in Figure 5c.

It was suggested that melittin peptides that are adsorbed on the bilayer surface do not reorient into a TM configuration.<sup>34</sup> Only those peptides that enter the membrane while they have a perpendicular to the surface orientation end up having a TM conformation. Thus, some of the melittin peptides can be in a state when they are in a configuration parallel to the surface and adsorbed to the membrane, and some can be perpendicular to the membrane surface, in the TM configurations.<sup>34</sup> To achieve this situation in simulations can take a rather long time, even in the coarse-grained simulations. Therefore, we considered two

additional simulations with the same P/L ratio as in case V-B, but we placed initially 6 of the melittin peptides in the transmembrane orientation. In system VI-Ba the TM peptides were placed further apart, with the separation between them 4 and 3 nm in the X and Y directions, respectively, while in system VI-Bb, the separations were 2 and 1.5 nm in the respective directions. The time evolution of these systems is shown in Figure 6. Again, no channels of well-defined shape were obtained. Figures 5b and 5c show snapshots of the side and top views of systems VI-Ba and VI-Bb at 2.0  $\mu$ s. From the figures we observe that again, like in case V-B, the assembly of peptides creates a hole, but not a channel, since some of the peptides in the assembly also have U-shaped configurations.

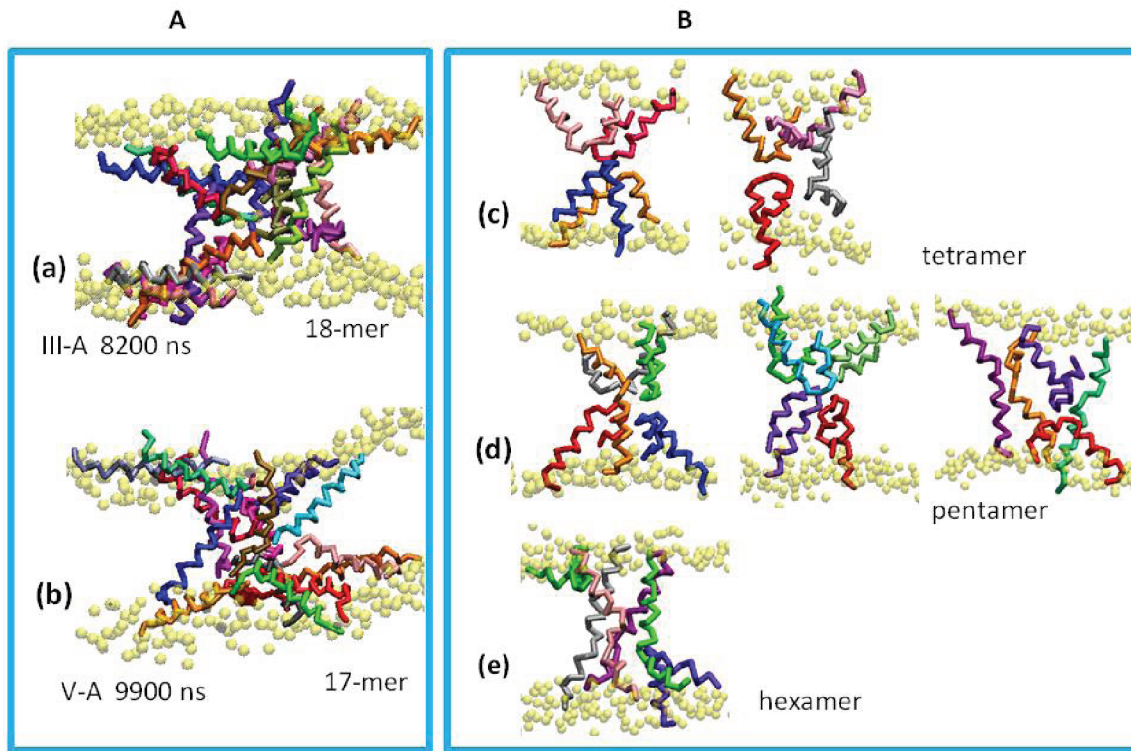


**Figure 7.** Transmembrane aggregates formed by magainin-2 (A) and melittin (B) in the simulations. (a) The pore aggregate formed after  $8.2 \mu\text{s}$  in system III-A. The aggregate contains as many as 18 peptides. (b) Pore aggregate in the symmetric case V-A after  $9.9 \mu\text{s}$  contained 17-peptides. Melittin aggregates are shown in (B). The aggregates are found to contain up to six peptides. (c), (d) and (e) show tetramers, pentamers, and hexamers found in simulations V-B, VI-Ba, and VI-Bb. The  $\text{PO}_4$  groups are shown as transparent yellow beads to indicate the position of the bilayer.

## ■ DISCUSSION AND CONCLUSIONS

Our simulations clearly show that actions of the antimicrobial peptides magainin-2 and melittin on lipid bilayers are substantially different. Magainin-2 forms water-filled toroidal pores, while we observed indications that melittin tends to micellize the bilayer when a large misbalance of peptides is present on the bilayer leaflets. When melittin peptides are present on both surfaces of the bilayer they form transmembrane aggregates that are not well-defined channels. In both cases III-A and V-A, top views of the systems from Figure 4 (4b and 4d) show that magainin-2 initiates creation of small holes in the bilayer, which keep on increasing in size with time as many peptides aggregate in the pore region. Notice that magainin-2 tends to aggregate in large numbers in the pore region. This creates large holes in the membranes and largely disrupts the membrane. At the same time, Figure 5c shows that melittin does not aggregate in large numbers inside the bilayer, and as a result, it creates smaller holes in the bilayer. Figure 7 compares the aggregates formed by both peptides in the pore region. Figures 7a and 7b show aggregates of magainin-2 in systems III-A and V-A, respectively. At  $8.2 \mu\text{s}$  of the run, as many as 18 magainin-2 peptides were associated with the pore in the system III-A, while 17 peptides were associated with the pore aggregate of system V-A at  $9.9 \mu\text{s}$ . Note that these peptides are arranged in a disordered fashion, mostly parallel, perpendicular, or tilted with respect to the surface of the bilayer. However, melittin aggregates were found to contain 4–6 peptides, and no further aggregation occurred. As a result, holes in bilayer due to melittin did not change size with time. Furthermore, melittins that are adsorbed on the surface of the bilayer seem to adopt mostly an U-shaped conformation with

its both termini ends attached to the same leaflet of the bilayer. Figures 7c, 7d, and 7e depict various melittin aggregates inside the bilayer obtained from systems V-B, VI-Ba, and VI-Bb. The figure shows tetramers, pentamers, and hexamers of peptides. We also found that peptides placed in a TM conformation retained it, while there is a probability for a peptide to move to a TM conformation from a conformation when they are parallel to the surface. Thus, in the system V-B, when peptides were initially placed parallel to the membrane plane, one of the peptides (out of 24) reoriented into a TM state.

The situation is very different for magainin-2. As mentioned previously, magainin-2 in system III-A creates pores by translocating to the side 2 of the bilayer. Figure 8a shows top view of the side 2 of the bilayer at different times. At 50 ns there is just one peptide on the side 2. As time progressed, more peptides translocated to side 2. Thus, at  $2.1 \mu\text{s}$  as many as 4 peptides (about 17% of the total number of peptides) were fully translocated to the side 2. However, no further translocation occurred, as indicated by the snapshot at  $8.2 \mu\text{s}$ .

Our CG simulations show that magainin-2 creates pores in phospholipid bilayers that are large enough to allow transport of water across them. Magainin-2 can also translocate across the bilayer indicating that pores are very flexible. In comparison, melittin adsorbed on the bilayer surface is even resistant to change into the TM orientation. The holes created by melittin in the bilayer were not found to be water-filled, as indicated by Figures 2, 5, and 6. However, Figure 8b shows that some permeation of water across the hole is possible, thus indicating that while magainin pores are large enough for molecules to pass through easily, melittin holes may allow permeation of small molecules, but at a low rate. These observations are

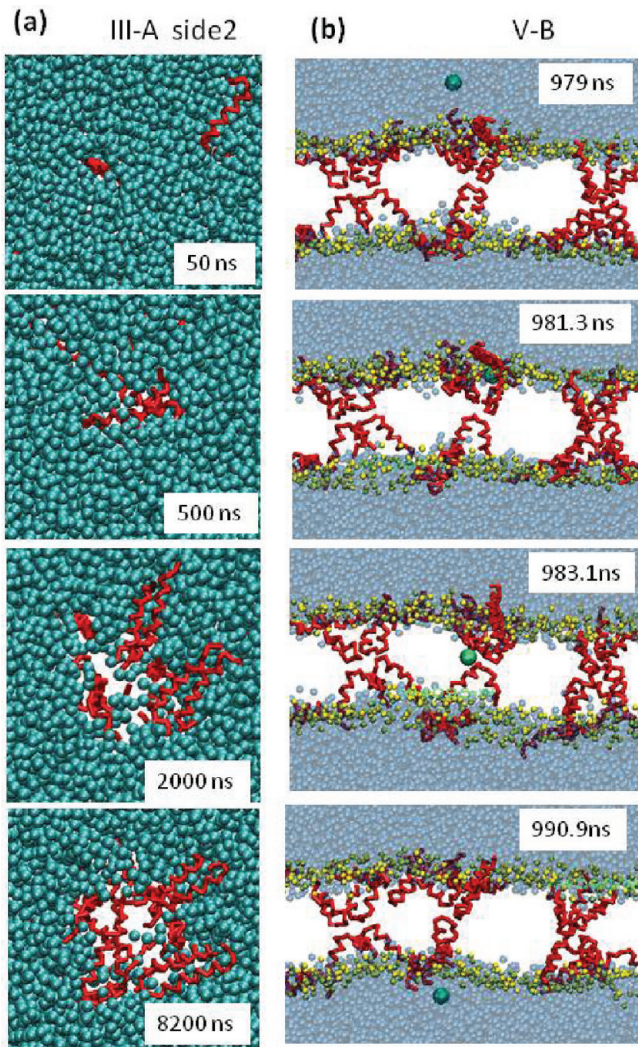


**Figure 8.** (a) Magainin-2 translocating across the bilayer in system III-A. By about  $2 \mu\text{s}$  as many as 4 peptides (about 17% of the total number of peptides) have translocated to side 2 of the bilayer. The DPPC molecules are represented by cyan beads and protein backbones are shown in red. (b) Melitin aggregates in the bilayer allow water to permeate small holes in the bilayer. The permeating water bead is enlarged and shown in green for clarity. Proteins are shown in red and other water molecules are shown as transparent blue beads, while the  $\text{PO}_4$  groups are shown as yellow beads.

consistent with the experimental finding that efflux of the dye from vesicles in solutions containing magainin-2 AMPs displays all-or-none kinetics, while in case of melittin the kinetics is graded.

We performed additional simulations on our systems starting with different initial conditions, although in all of them peptides were located close to the headgroup/tail interface of the lipid bilayer. In all cases we observed results qualitatively similar to the ones reported above.

Why is there such a difference between the actions of the two AMPs: magainin-2 and melittin? The answer to this question can be seen in the difference of the specific amino acid sequences of the two peptides. The presence of the proline residue in melittin allows it to attain an U-shaped conformation, which is stabilized by anchoring positively charged peptide termini to interfacial region of the membranes that contain negatively charged phosphate groups. This is not the

case for magainin-2. We believe that the peptide–peptide interactions also play an important role in the assembly of peptides in the membrane. Since the total charge of magainin-2 is smaller, the peptides will easier self-assemble into aggregates. By creating toroidal pores, the close contacts between peptides are avoided. The observed misalignment of magainin peptides in our simulations also helps in reducing charge–charge interaction. In the case of melittin, it is the U-shaping of the peptides that effectively reduces charge–charge interaction.

More simulations, both on coarse-grained and molecular-detailed levels, are needed to study the effect of peptide–peptide interactions. Our present coarse-grained simulations showed that the structures of peptide assemblies are consistent with the observed all-or-none kinetics of the dye efflux from vesicles when exposed to solution containing magainin-2, while in the case of melittin the kinetics is graded.

## ■ AUTHOR INFORMATION

### Notes

The authors declare no competing financial interest.

## ■ ACKNOWLEDGMENTS

This work was supported by the National Science Foundation under Grant MCB-0950280. We thank Dr. Sheeba J. Irudayam for a careful reading of the manuscript and for providing useful suggestions.

## ■ REFERENCES

- Wimley, W. C.; Hristova, K. *J. Membr. Biol.* **2011**, *239*, 27.
- Ehrenstein, G.; Lecar, H. *Q. Rev. Biophys.* **1977**, *10*, 1.
- Ludtke, S. J.; He, K.; Heller, W. T.; Harroun, T. A.; Yang, L.; Huang, H. W. *Biochemistry* **1996**, *35*, 13723.
- Pokorny, A.; Birkbeck, T. H.; Almeida, P. F. F. *Biochemistry* **2002**, *41*, 11044.
- Shai, Y. *Biopolymers* **2002**, *66*, 236.
- Qian, S.; Wang, W. C.; Yang, L.; Huang, H. W. *Proc. Natl. Acad. Sci. U. S. A.* **2008**, *105*, 17379.
- Almeida, P. F.; Pokorny, A. *Biochemistry* **2009**, *48*, 8083.
- Yang, L.; Harroun, T. A.; Weiss, T. M.; Ding, L.; Huang, H. W. *Biophys. J.* **2001**, *81*, 1475.
- Sengupta, D.; Leontiadou, H.; Mark, A. E.; Marrink, S. J. *Biochim. Biophys. Acta, Biomembr.* **2008**, *1778*, 2308.
- Clark, K. S.; Svetlovics, J.; McKeown, A. N.; Huskins, L.; Almeida, P. F. *Biochemistry* **2011**, *50*, 7919.
- Leontiadou, H.; Mark, A. E.; Marrink, S. J. *J. Am. Chem. Soc.* **2006**, *128*, 12156.
- Manna, M.; Mukhopadhyay, C. *Langmuir* **2009**, *25*, 12235.
- Mihajlovic, M.; Lazaridis, T. *Biochim. Biophys. Acta, Biomembr.* **2010**, *1798*, 1485.
- Irudayam, S. J.; Berkowitz, M. L. *Biochim. Biophys. Acta, Biomembr.* **2011**, *1808*, 2258.
- Lindorff-Larsen, K.; Piana, S.; Dror, R. O.; Shaw, D. E. *Science* **2011**, *334*, 517.
- Marrink, S. J.; Risselada, H. J.; Yefimov, S.; Tieleman, D. P.; de Vries, A. H. *J. Phys. Chem. B* **2007**, *111*, 7812.
- Monticelli, L.; Kandasamy, S. K.; Periole, X.; Larson, R. G.; Tieleman, D. P.; Marrink, S. J. *J. Chem. Theory Comput.* **2008**, *4*, 819.
- Rzepiela, A. J.; Sengupta, D.; Goga, N.; Marrink, S. J. *Faraday Discuss.* **2010**, *144*, 431.
- Gkeka, P.; Sarkisov, L. *J. Phys. Chem. B* **2010**, *114*, 826.
- Woo, H. J.; Wallqvist, A. *J. Phys. Chem. B* **2011**, *115*, 8122.
- Raghuraman, H.; Chattopadhyay, A. *Biosci. Rep.* **2007**, *27*, 189.
- Van der Spoel, D.; Lindahl, E.; Hess, B.; Groenhof, G.; Mark, A. E.; Berendsen, H. J. C. *J. Comput. Chem.* **2005**, *26*, 1701.
- Hristova, K.; Dempsey, C. E.; White, S. H. *Biophys. J.* **2001**, *80*, 801.

- (24) Matsuzaki, K. *Biochim. Biophys. Acta, Biomembr.* **1999**, *1462*, 1.  
(25) Terwilliger, T. C.; Eisenberg, D. *J. Biol. Chem.* **1982**, *257*, 6010.  
(26) Terwilliger, T. C.; Eisenberg, D. *J. Biol. Chem.* **1982**, *257*, 6016.  
(27) Gesell, J.; Zasloff, M.; Opella, S. J. *J. Biomol. NMR* **1997**, *9*, 127.  
(28) Berendsen, H. J. C.; Postma, J. P. M.; Vangunsteren, W. F.;  
Dinola, A.; Haak, J. R. *J. Chem. Phys.* **1984**, *81*, 3684.  
(29) Parrinello, M.; Rahman, A. *J. Appl. Phys.* **1981**, *52*, 7182.  
(30) Humphrey, W.; Dalke, A.; Schulten, K. *J. Mol. Graphics* **1996**,  
*14*, 33.  
(31) Dempsey, C. E.; Ueno, S.; Avison, M. B. *Biochemistry* **2003**, *42*,  
402.  
(32) Tamba, Y.; Yamazaki, M. *J. Phys. Chem. B* **2009**, *113*, 4846.  
(33) Yeh, I. C.; Olson, M. A.; Lee, M. S.; Wallqvist, A. *Biophys. J.* **2008**, *95*, 5021.  
(34) van den Bogaart, G.; Guzman, J. V.; Mika, J. T.; Poolman, B. *J. Biol. Chem.* **2008**, *283*, 33854.